Electronic Supplementary Material (ESI) for Dalton Transactions.

Supplementary Information

Discriminatory behavior of a rhodamine 6G decorated mesoporous silica based multiple cation sensor towards Cu^{2+} and Hg^{2+} *vis-à-vis* Al^{3+}, Cr^{3+} and Fe^{3+}: Selective removal of Cu^{2+} and Hg^{2+} from aqueous medium

Debdas Singha,[a] Ananya Pal,[a] Hiroshi Uyama,[b] Partha Roy,[c] Mahasweta Nandi*,[a]

[a]*Integrated Science Education and Research Centre, Siksha Bhavana, Visva-Bharati University, Santiniketan 731 235, India*

Email: mahasweta.nandi@visva-bharati.ac.in

[b]*Department of Applied Chemistry, Graduate School of Engineering, Osaka University, 2-1 Yamadaoka, Suita, Osaka, 565-0871, Japan*

[c]*Department of Chemistry, Jadavpur University, Kolkata 700032, India*

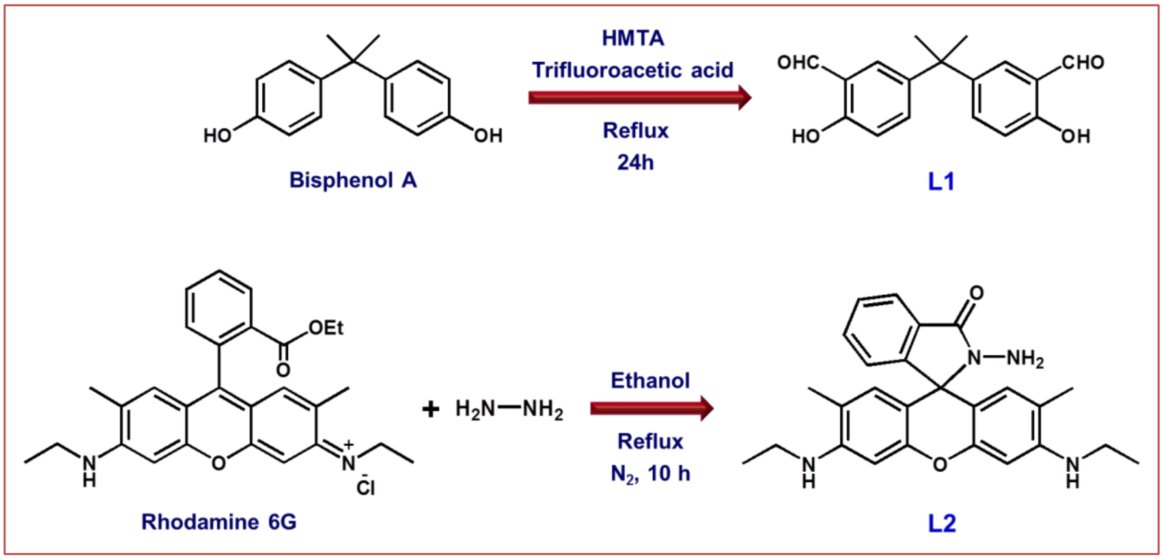

Scheme S1. Syntheses of **L1** and **L2**

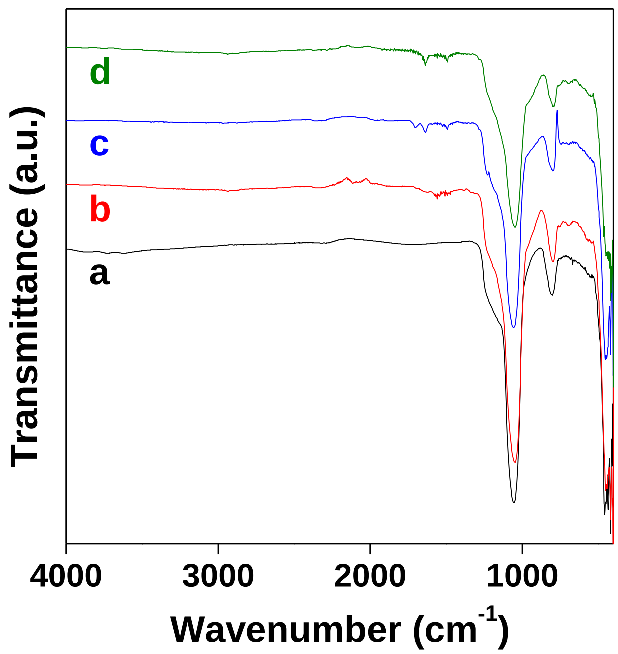

Fig. S1. FT-IR spectra of (a) mesoporous silica (**MS**), (b) **3-APTES-FMS**, (c) **CHO-FMS** and (d) **R6FMS**.

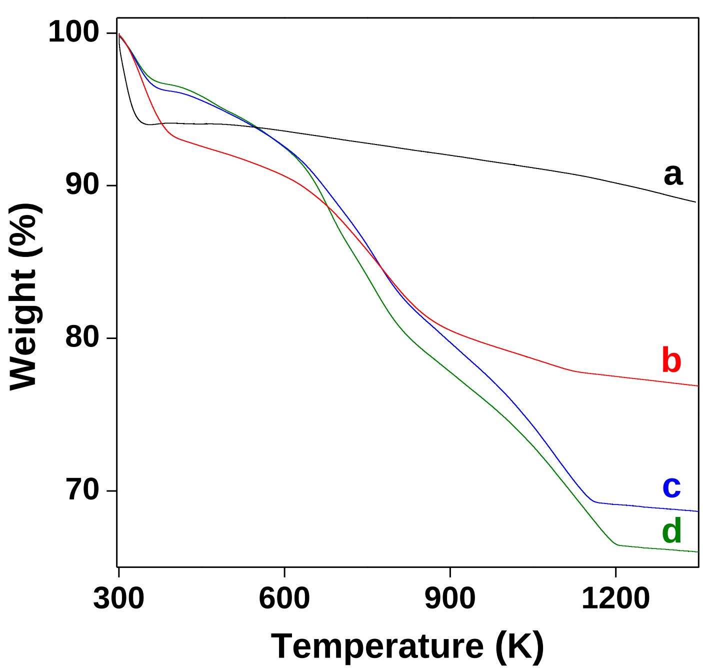

Fig. S2. Thermogravimetric analysis of (a) mesoporous silica (**MS**), (b) **3-APTES-FMS**, (c) **CHO-FMS** and (d) **R6FMS**.

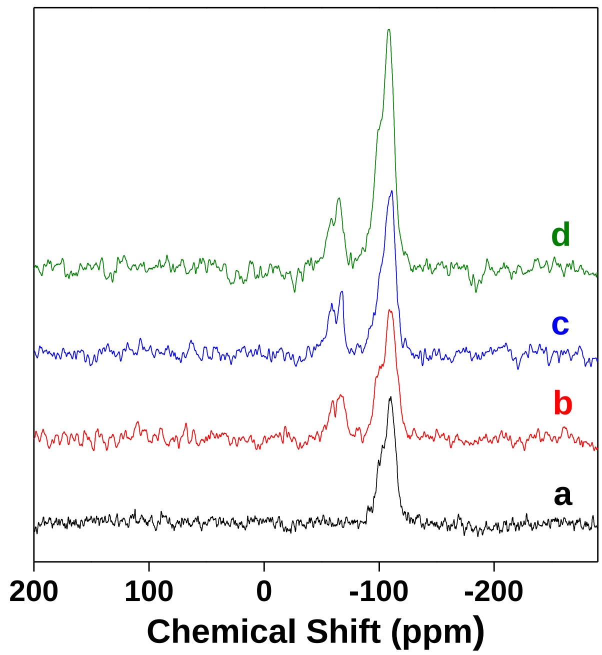

Fig. S3. Solid state ^{29}Si MAS NMR spectra of (a) mesoporous silica (**MS**), (b) **3-APTES-FMS**, (c) **CHO-FMS** and (d) **R6FMS**.

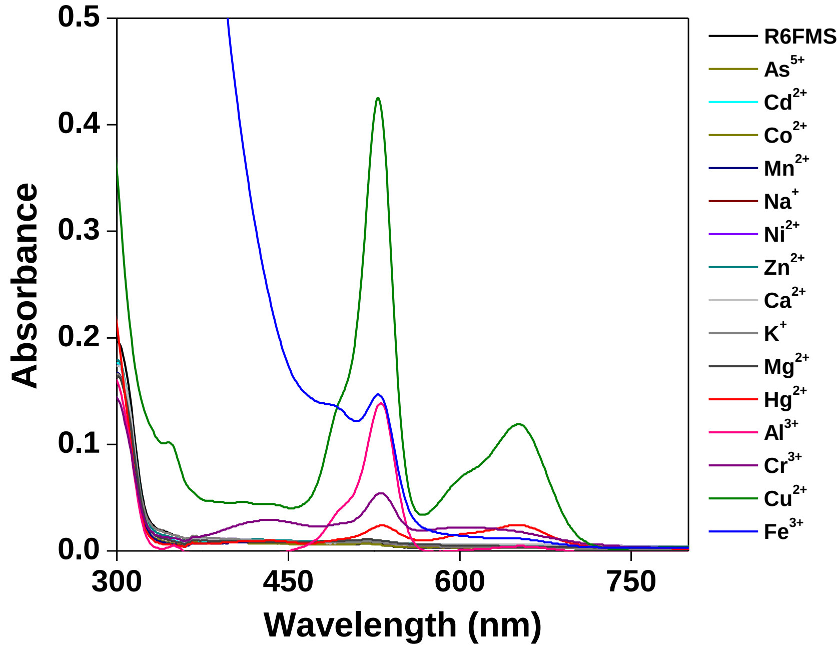

Fig. S4. Absorption spectra of **R6FMS** in the presence of 800 µM of different metal ions (for Cu^{2+}: 500 µM) in ethanol at 298 K (*l* = 1 cm).

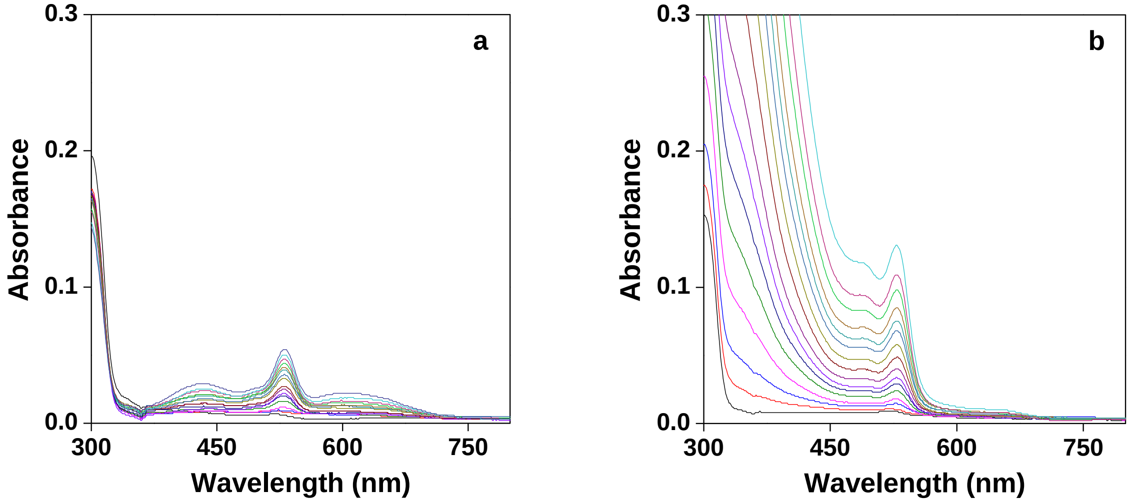

Fig. S5. Absorption spectra of **R6FMS** in the presence of (0-800 μM) (a) Cr^{3+} and (b) Fe^{3+} in ethanol at 298 K (l = 1 cm).

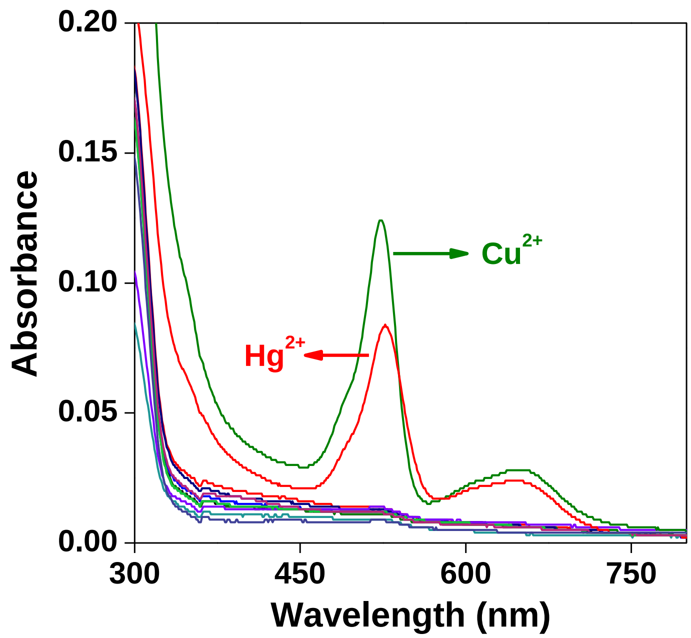

Fig. S6. Absorption spectra of **R6FMS** in the presence 800 μM concentration of different metal ions in 10 mM HEPES buffer in water/acetonitrile = 14:1 (v/v) (pH 7.2) at 298 K (l = 1 cm).

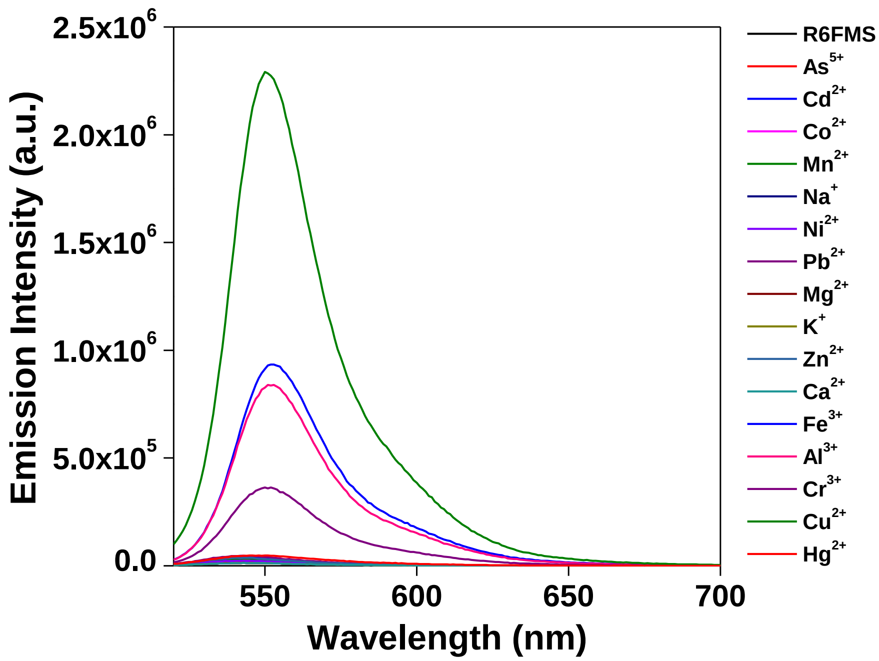

Fig. S7. Fluorescence spectra of **R6FMS** in the presence 800 μM of different metal ions in ethanol at 298 K.

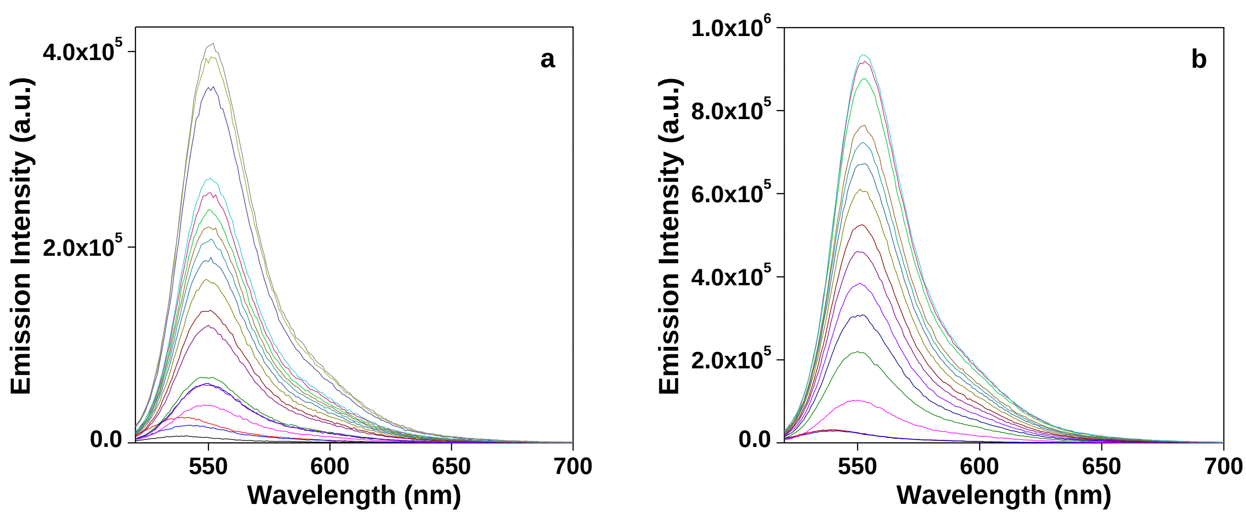

Fig. S8. Fluorescence spectra of **R6FMS** in the presence of different concentrations of (a) Cr^{3+} (0-800 μM) and (b) Fe^{3+} (0-800 μM) in ethanol at 298 K.

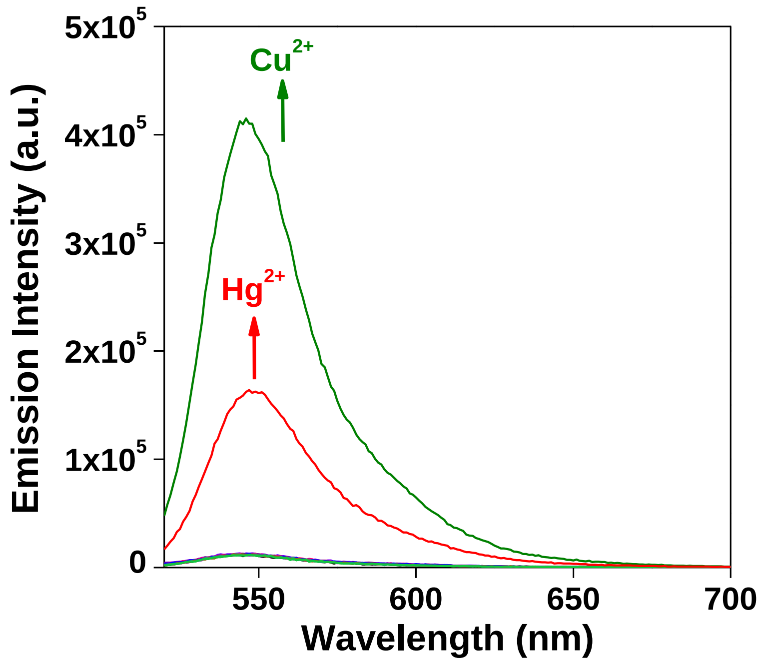

Fig. S9. Fluorescence spectra of **R6FMS** in the presence of 800 μM of all metal ions in 10 mM HEPES buffer in water/acetonitrile = 14:1 (v/v) (pH 7.2) at 298 K.

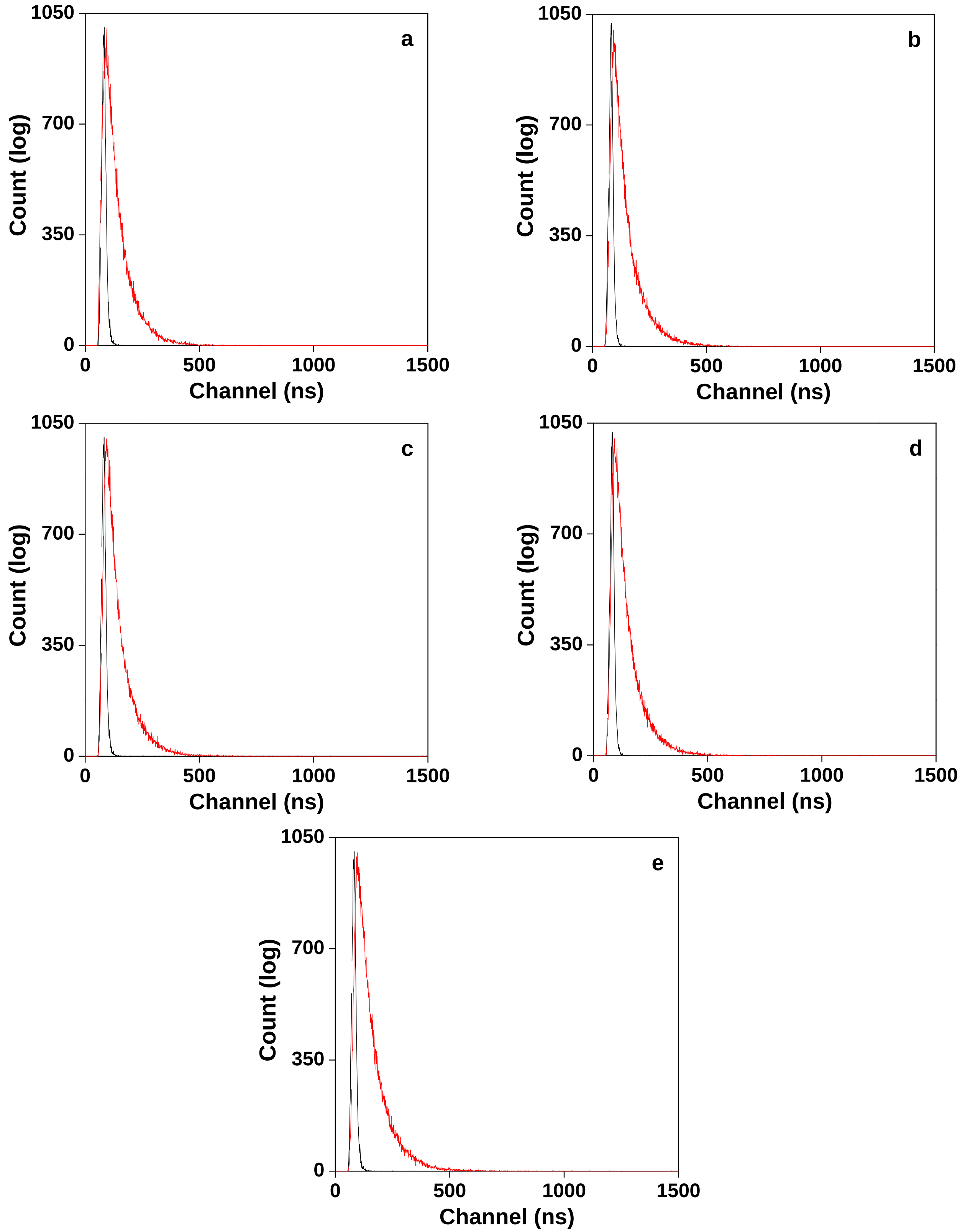

Fig. S10. Excited state fluorescence decay behavior of (a) **R6FMS** and its complex with (b) Al^{3+}, (c) Cr^{3+}, (d) Fe^{3+} and (e) Cu^{2+} ions in ethanol at 298 K.

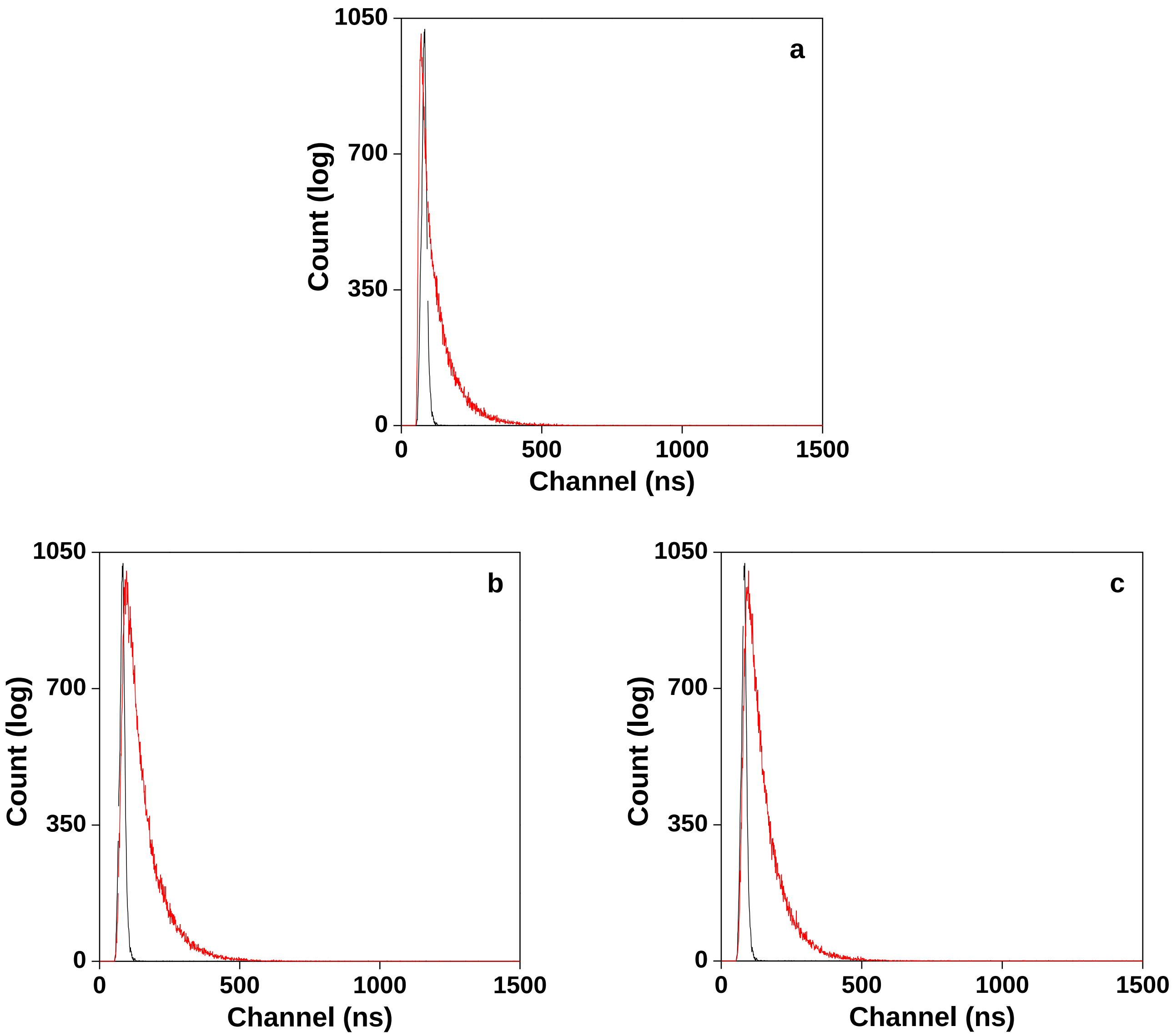

Fig. S11. Excited state fluorescence decay behavior of (a) **R6FMS** and its complex with (a) Cu^{2+} and (c) Hg^{2+} ions in 10 mM HEPES buffer in water/acetonitrile = 14:1 (v/v) (pH 7.2) at 298 K.

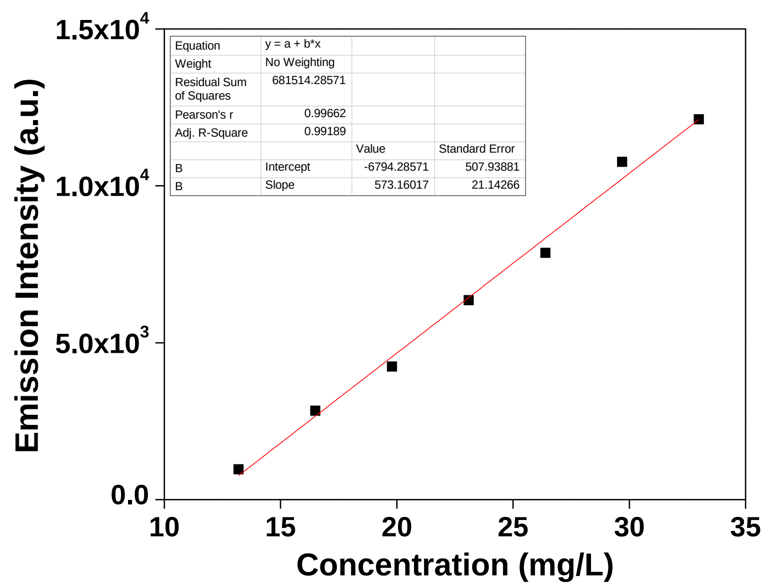

Fig. S12. Determination of Sb1 of the blank, **R6FMS** in ethanol at 298 K.

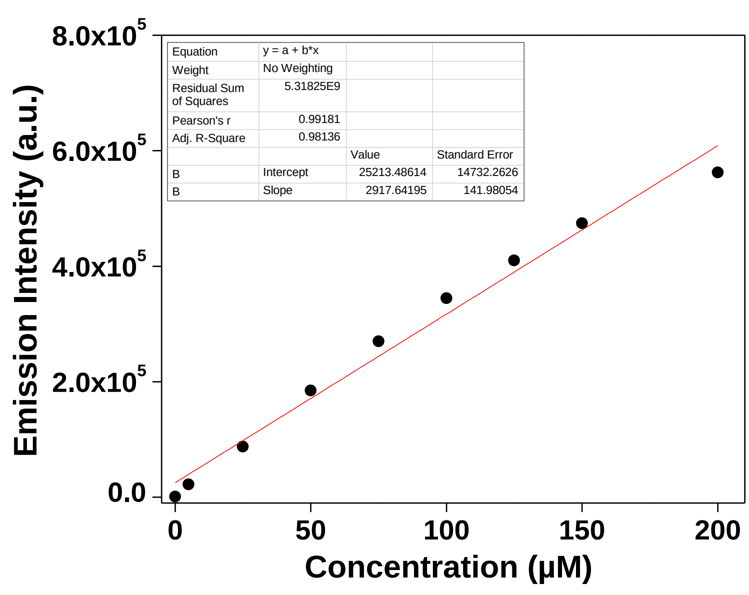

Fig. S13. Linear dynamic plot of F.I. (at 552 nm) *vs.* [Al^{3+}] in ethanol for the determination of S (slope).

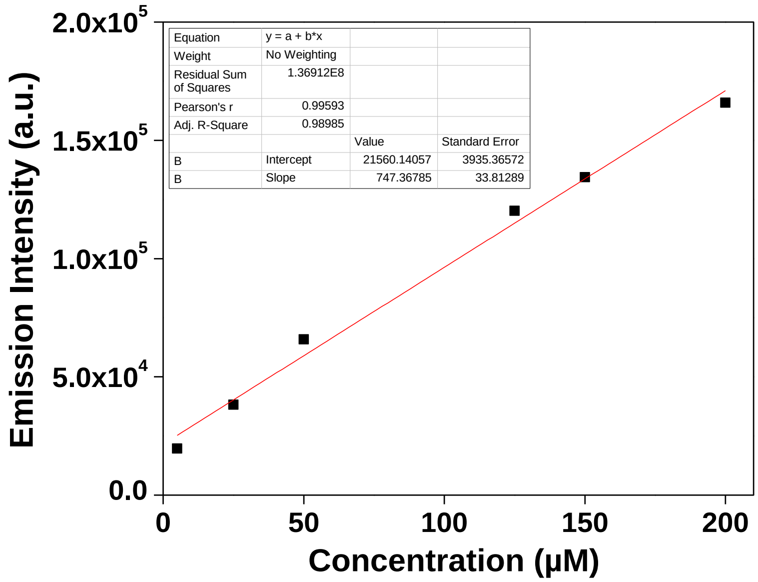

Fig. S14. Linear dynamic plot of F.I. (at 552 nm) *vs.* [Cr^{3+}] in ethanol for the determination of S (slope).

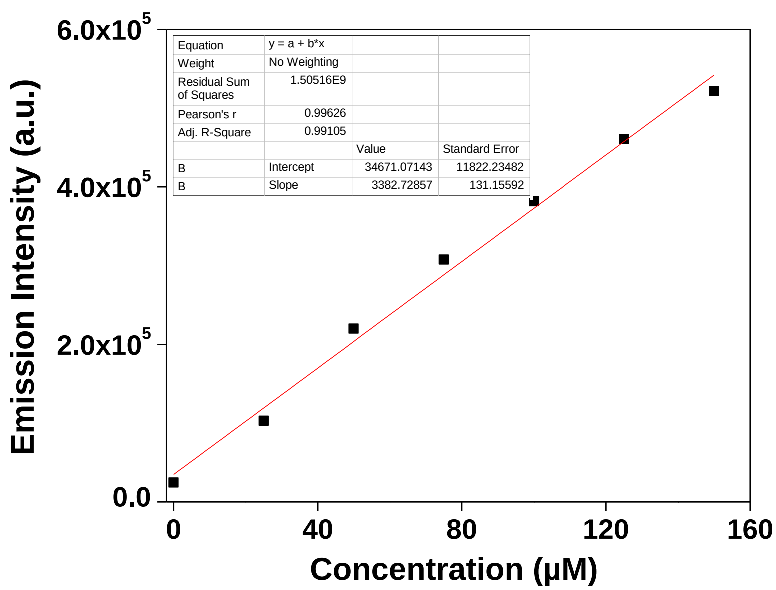

Fig. S15. Linear dynamic plot of F.I. (at 552 nm) *vs.* [Fe^{3+}] in ethanol for the determination of S (slope).

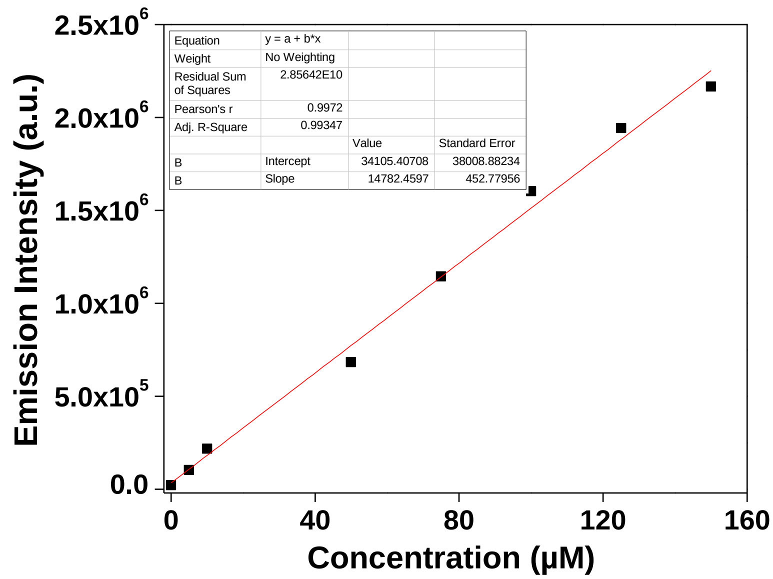

Fig. S16. Linear dynamic plot of F.I. (at 552 nm) *vs.* $[Cu^{2+}]$ in ethanol for the determination of S (slope).

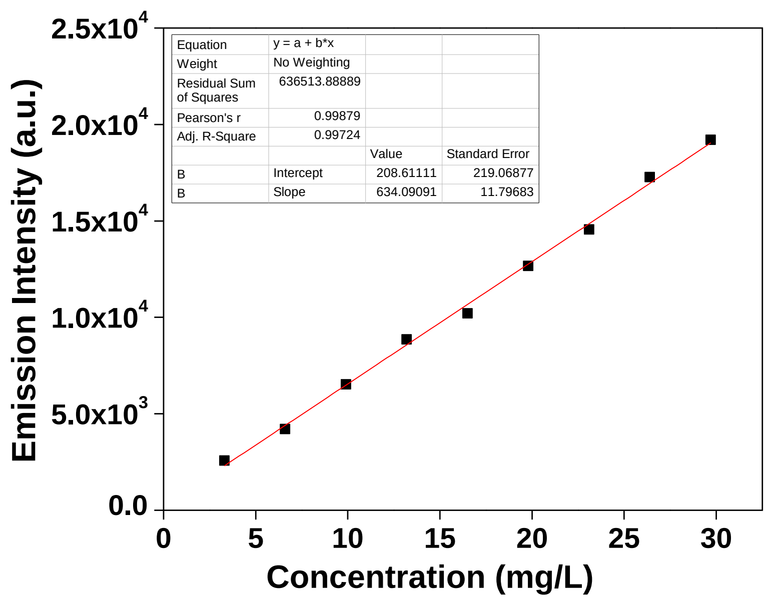

Fig. S17. Determination of Sb1 of the blank, **R6FMS** in water/acetonitrile (14:1, v/v) (pH 7.2, HEPES buffer) at 298 K.

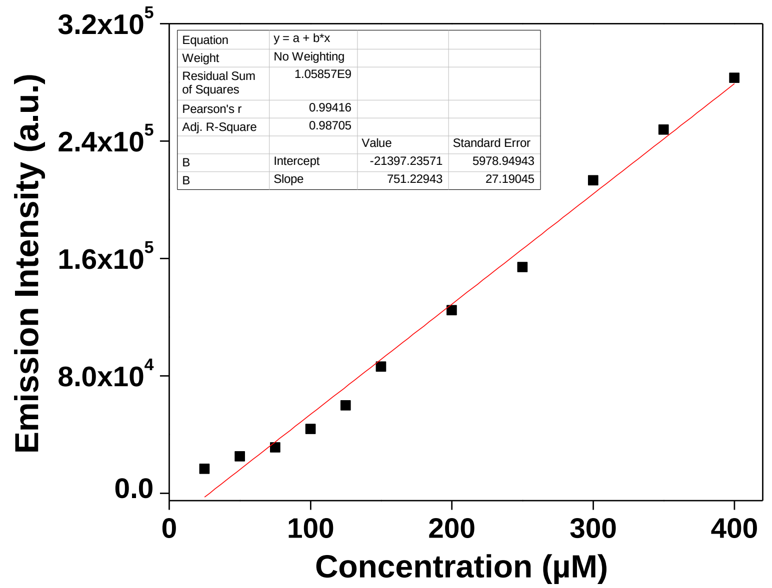

Fig. S18. Linear dynamic plot of F.I. (at 552 nm) *vs.* [Cu^{2+}] for the determination of S (slope) in water/acetonitrile (14:1, v/v) (pH 7.2, HEPES buffer).

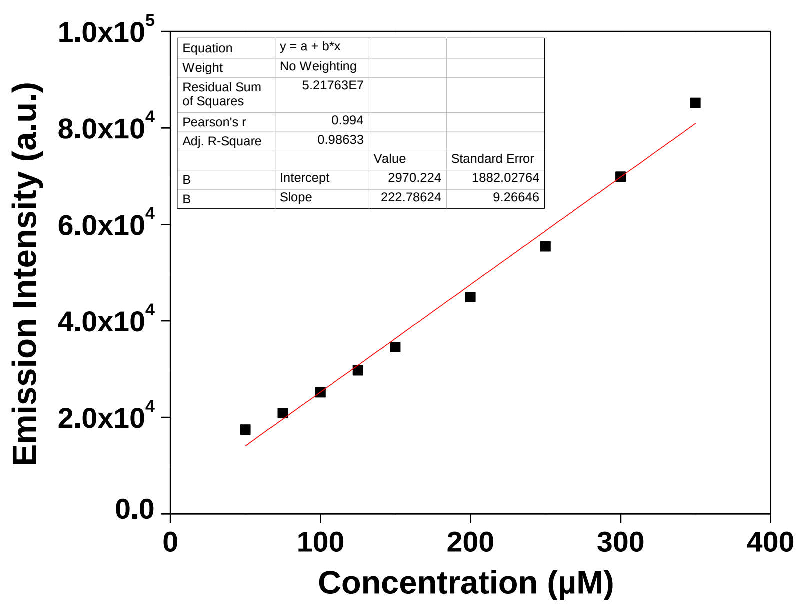

Fig. S19. Linear dynamic plot of F.I. (at 552 nm) *vs.* [Hg^{2+}] for the determination of S (slope) in water/acetonitrile (14:1, v/v) (pH 7.2, HEPES buffer).

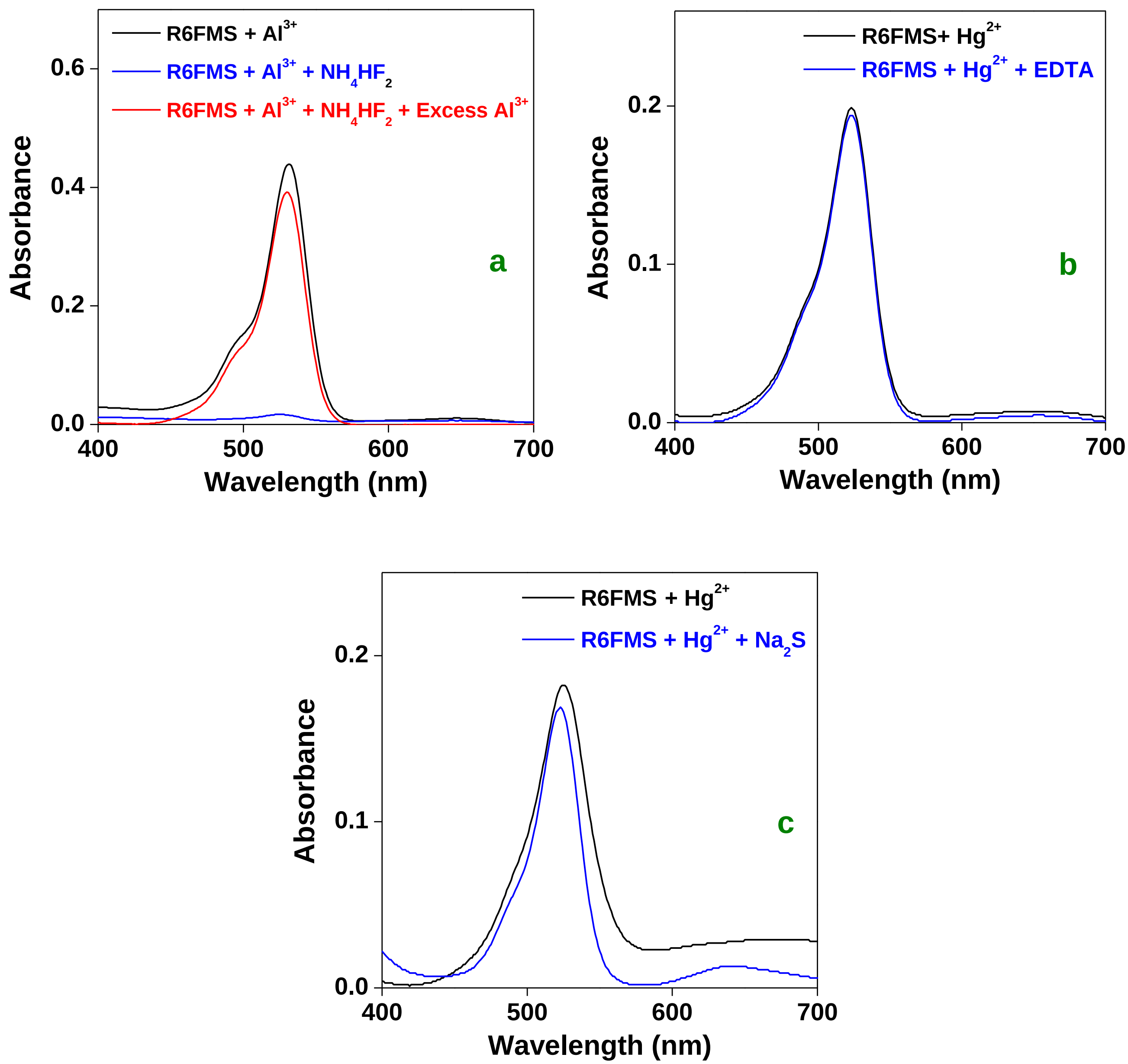

Fig. S20. Absorbance of **R6FMS** in the presence of Al^{3+} and Hg^{2+} with different complexing agents. (a) Reversibility test of Al^{3+} binding with **R6FMS** in the presence F^- ion in ethanol indicating reversible binding nature of aluminum, (b) Reversibility test of Hg^{2+} binding with **R6FMS** in the presence of Na_2-EDTA in water/acetonitrile (14:1, v/v) (pH 7.2, HEPES buffer) and (c) Reversibility test of Hg^{2+} binding with **R6FMS** in the presence of Na_2S in water/acetonitrile (14:1, v/v) (pH 7.2, HEPES buffer). Both the tests (b and c) indicate that the binding of Hg^{2+} with the probe is not reversible.

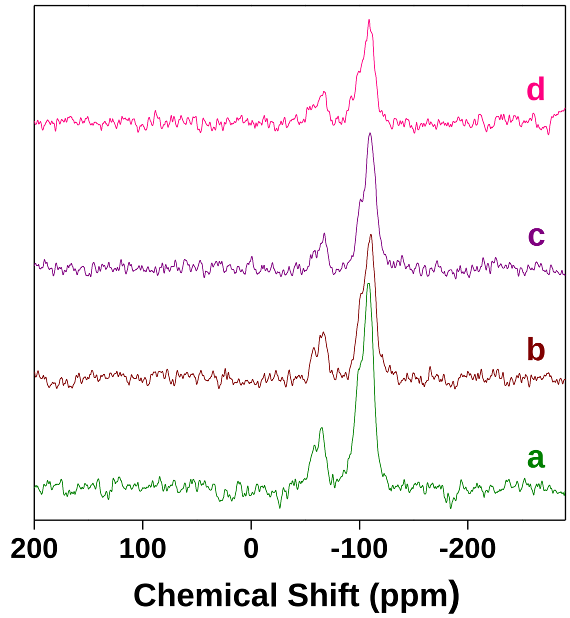

Fig. S21. Solid state ^{29}Si MAS NMR spectra of (a) **R6FMS**, (b) Al^{3+}-**R6FMS** in ethanol, (c) Hg^{2+}-**R6FMS** in ethanol and (d) Hg^{2+}-**R6FMS** in HEPES buffer in water/acetonitrile.

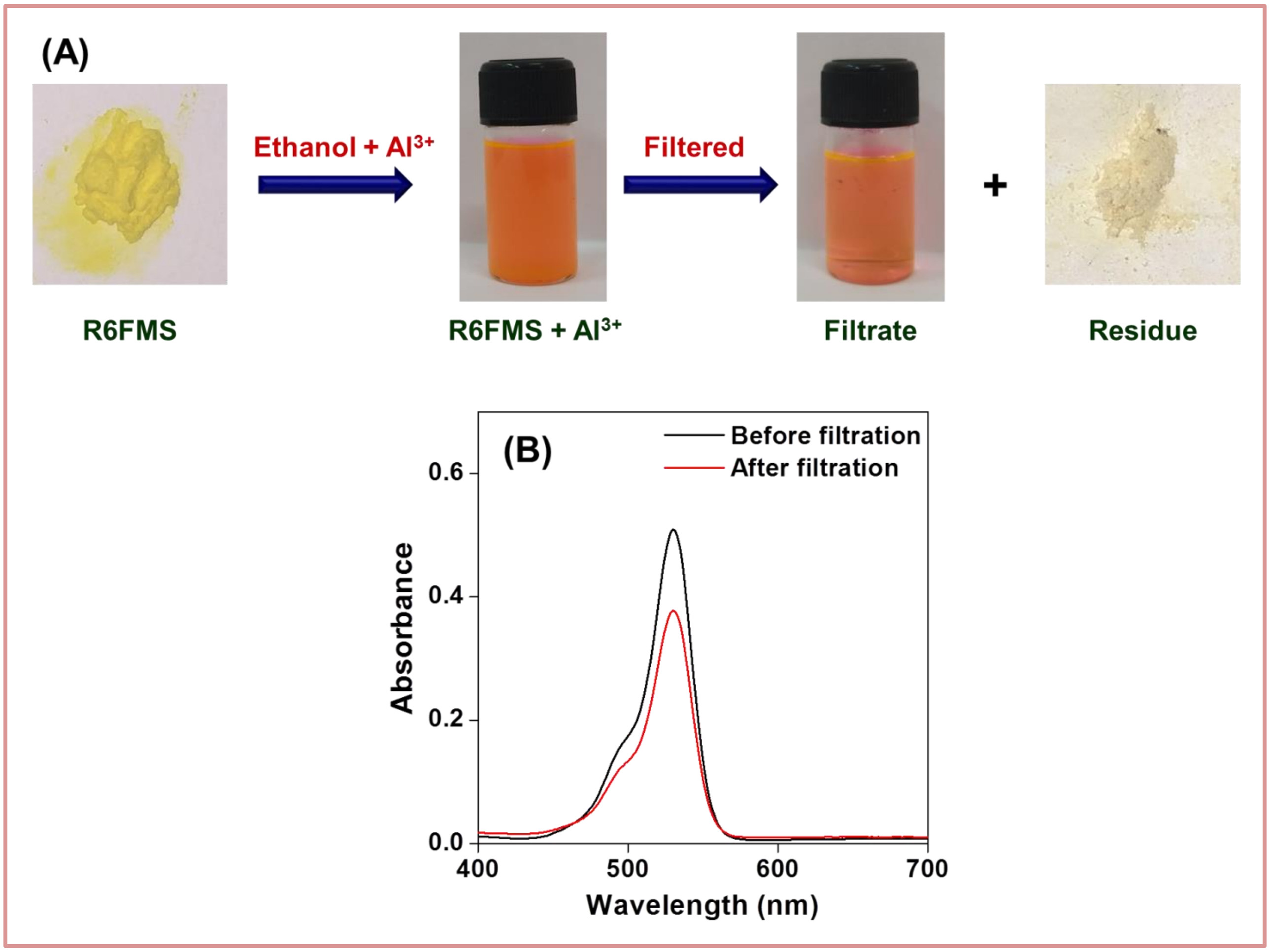

Fig. S22. (A) Change of color of **R6FMS** in the presence of Al^{3+} in ethanol before and after filtration and (B) Absorption spectra of **R6FMS** in the presence of Al^{3+} ion in ethanol before and after filtration.

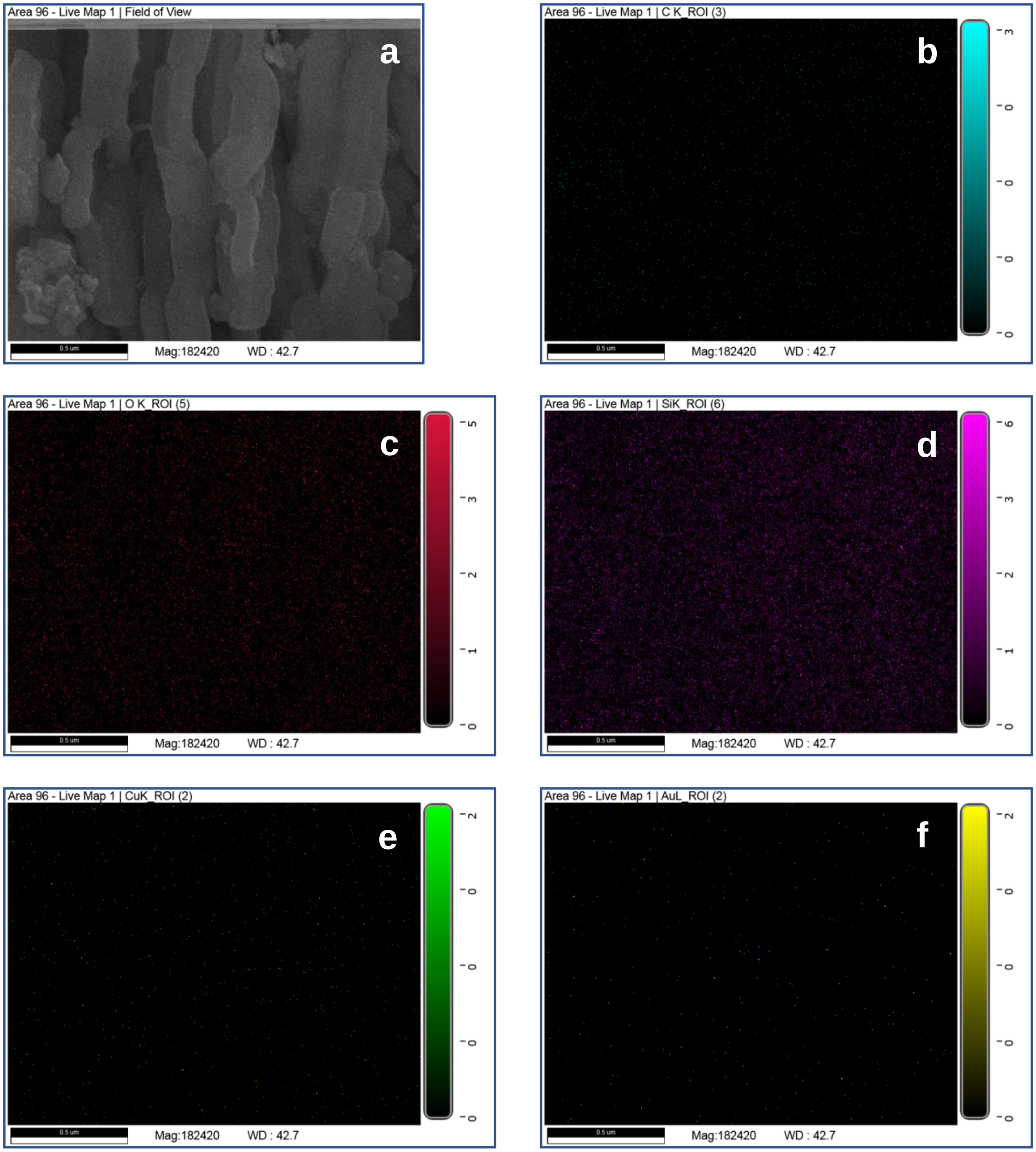

Fig. S23. (a) Area selected for EDS spectrum and corresponding EDS patterns showing elemental mapping in Cu^{2+}-**R6FMS** of (b) Carbon (cyan), (c) Oxygen (red), (d) Silicon (magenta), (e) Copper (green) and (f) Gold (yellow).

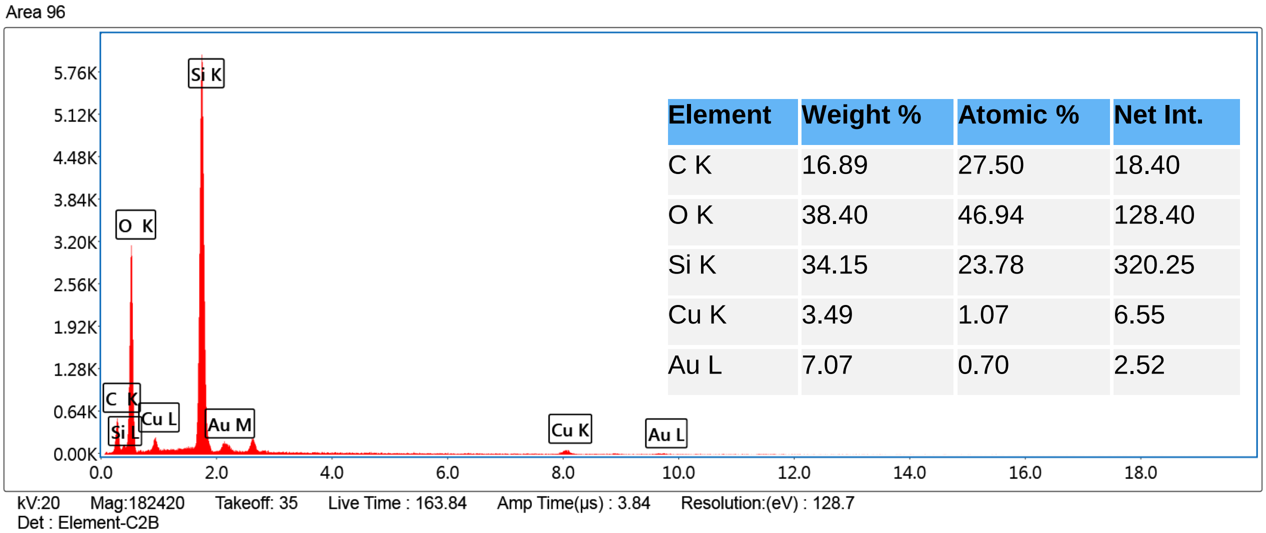

Fig. S24. EDS sum spectrum of Cu^{2+}-**R6FMS** showing the presence of the different elements on the sample surface.

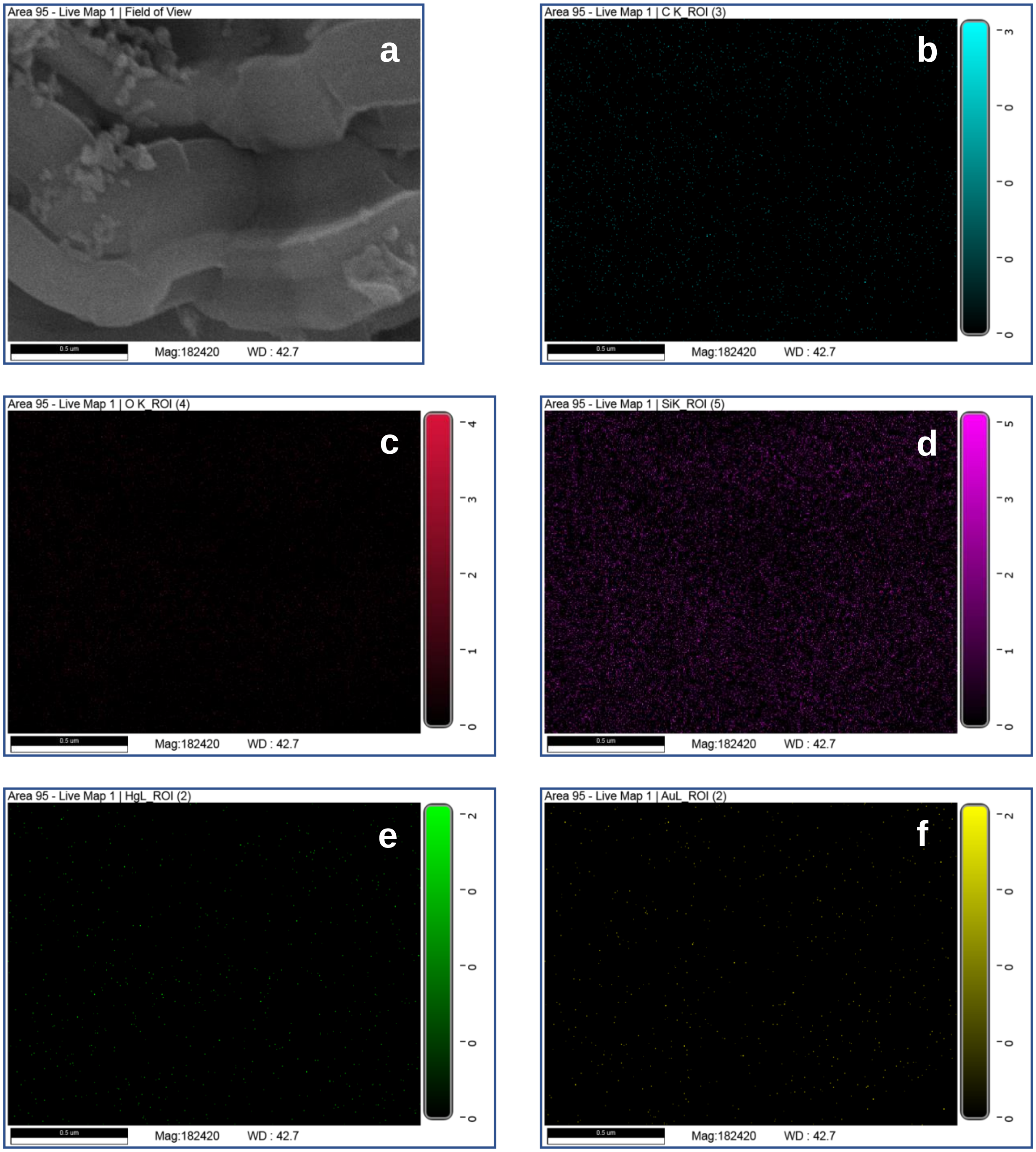

Fig. S25. (a) Area selected for EDS spectrum and corresponding EDS patterns showing elemental mapping in Cu^{2+}-**R6FMS** of (b) Carbon (cyan), (c) Oxygen (red), (d) Silicon (magenta), (e) Mercury (green) and (f) Gold (yellow) and (g) EDS sum spectrum of Hg^{2+}-**R6FMS** showing the presence of the different elements on the sample surface.

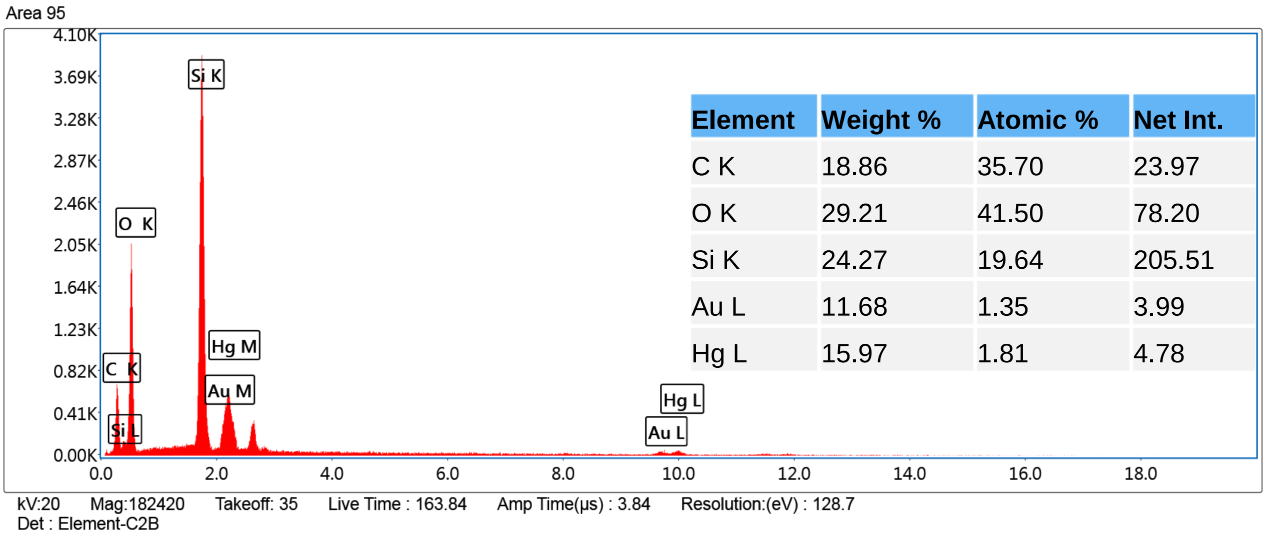

Fig. S26. EDS sum spectrum of Hg^{2+}-**R6FMS** showing the presence of the different elements on the sample surface.

Table S1. Solubility of different metal salts in water and ethanol at 25°C

No.	Formula	Solubility in water (g/L)	Solubility in ethanol (g/L)	Purchased from
1.	$NaCl$	360	0.65	Merck
2.	$MgCl_2$	543	74	Merck
3.	$Al(NO_3)_3.9H_2O$	739	86.3	Merck
4.	KCl	339.7	0.0029	Merck
5.	$CaCl_2$	811	258	Merck
6.	$CrCl_3.6H_2O$	585	---	Merck
7.	$MnCl_2.4H_2O$	739	74	Merck
8.	$FeCl_3$	912	830	Merck
9.	$CoCl_2.6H_2O$	529	86	Merck
10.	$NiCl_2.6H_2O$	675	8	Merck
11.	$CuCl_2.2H_2O$	757	530	Merck
12.	$ZnCl_2$	4320	4300	Merck
13.	$NaAsO_2$	1560	---	Merck
14.	$CdCl_2$	1196	14.8	Merck
15.	$HgCl_2$	69	40	Merck
16.	$Pb(NO_3)_2$	597	87.7	Merck

Speciation of metal ions

Literature study suggests the following species may exist under the experimental conditions in aqueous medium

Al^{3+} → $[Al(OH)(H_2O)_5]^{2+}$ and/or $[Al(OH)_2(H_2O)_4]^+$

Cr^{3+} → $Cr(OH)^{2+}$, $Cr(OH)_3$

Fe^{3+} → $[Fe(OH_2)_4Cl_2]^+$

Cu^{2+} → $CuCl^+$

Hg^{2+} → HgOHCl(aq)

References

1. G. Berthon, *Coord. Chem. Rev.*, 1996, **149**, 241-280.

2. R. Rakhunde, L. Deshpande and H. D. Juneja, *Crit. Rev. Env. Sci. Tec.*, 2012, **42**, 776-810.

3. S. A. Cotton, *J Coord. Chem.*, 2018, **71**, 3415-3443.

4. K. J. Powell, P. L. Brown, R. H. Byrne, T. Gajda, G. Hefter, S. Sjöberg and H. Wanner, *Pure Appl. Chem.*, 2007, **79**, 895-950.

5. K. J. Powell1, P. L. Brown, R. H. Byrne, T. Gajda, G. Hefter, S. Sjöberg and H. Wanner, *Pure Appl. Chem.*, 2005, **77**, 739-800.